4-Oxalocrotonate Tautomerase, Its Homologue YwhB, and Active Vinylpyruvate Hydratase: Synthesis and Evaluation of 2-Fluoro Substrate Analogues†

William H. Johnson, Jr.,§ Susan C. Wang,§ Thanuja M. Stanley,§ Robert M. Czerwinski,§ Jeffrey J. Almrud,§ Gerrit J. Poelarends,§ Alexey G. Murzin,‡ and Christian P. Whitman*,§

Division of Medicinal Chemistry, College of Pharmacy, The University of Texas, Austin, Texas 78712-1071, and MRC Centre for Protein Engineering, Hills Road, Cambridge CB2 2QH, U.K.

Received March 15, 2004; Revised Manuscript Received June 4, 2004

ABSTRACT: A series of 2-fluoro-4-alkene and 2-fluoro-4-alkyne substrate analogues were synthesized and examined as potential inhibitors of three enzymes: 4-oxalocrotonate tautomerase (4-OT) and vinylpyruvate hydratase (VPH) from the catechol meta-fission pathway and a closely related 4-OT homologue found in *Bacillus subtilis* designated YwhB. All of the compounds were potent competitive inhibitors of 4-OT with the monocarboxylated 2*E*-fluoro-2,4-pentadienoate and the dicarboxylated 2*E*-fluoro-2-en-4-ynoate being the most potent. Despite the close mechanistic and structural similarities between 4-OT and YwhB, these compounds were significantly less potent inhibitors of YwhB with K_i values ranging from 5- to 633-fold lower than those determined for 4-OT. The study of VPH is complicated by the fact that the enzyme is only active as a complex with the metal-dependent 4-oxalocrotonate decarboxylase (4-OD), the enzyme following 4-OT in the catechol meta-fission pathway. A structure-based sequence analysis identified 4-OD as a member of the fumarylacetoacetate hydrolase (FAH) superfamily and implicated Glu-109 and Glu-111 as potential metal-binding ligands. Changing these residues to a glutamine verified their importance for enzymatic activity and enabled the production of soluble E109Q4-OD/VPH or E111Q4-OD/VPH complexes, which retained full hydratase activity but had little decarboxylase activity. Subsequent incubation of the E109Q4-OD/VPH complex with the substrate analogues identified the 2*E* and 2*Z* isomers of the monocarboxylated 2-fluoropent-2-en-4-ynoate as competitive inhibitors. The combined results set the stage for crystallographic studies of 4-OT, YwhB, and VPH using these inhibitors as ligands.

Several microorganisms are able to use various aromatic hydrocarbons as their sole sources of carbon and energy due to the presence of catabolic pathways that convert these compounds to intermediates, which can be channeled into the Krebs cycle (*1*, *2*). One of these pathways, the catechol meta-fission pathway, is replete with chemically intriguing intermediates as well as interesting enzymes and structures (*1*−*3*). In the course of this pathway, several dienols of varying reactivity are generated, including 2-hydroxy-2,4-hexadienedioate (**1**, Scheme 1) and 2-hydroxy-2,4-pentadienoate (**2**). In aqueous buffer, both dienols rapidly ketonize to their respective β,γ-unsaturated ketones (**3** and **4**, Scheme 1) before a much slower conversion to the α,β-unsaturated ketones (**5** and **6**, Scheme 1) (*4*, *5*). At equilibrium, **5** and **6** predominate. In the catechol meta-fission pathway, **1** serves as a substrate for 4-oxalocrotonate tautomerase (4-OT)[1] (*4*), while **2** is generated by the 4-oxalocrotonate decarboxylase (4-OD)-catalyzed decarboxylation of 2-oxo-3-hexenedioate (**5**, Scheme 2) (*6*) and is subsequently processed by vinylpyruvate hydratase (VPH) to form 2-oxo-(4*S*)-hydroxypentanoate (**7**, Scheme 2) (*7*). 4-OD and VPH exist as a multienzyme complex, in which both require either Mn^{2+} or Mg^{2+} for activity (*2*).

Scheme 1

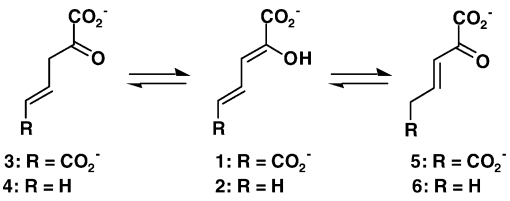

Scheme 2

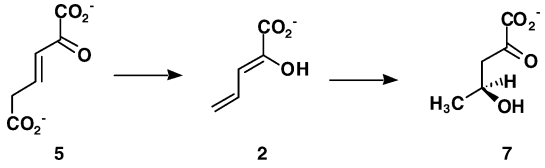

† This research was supported by the National Institutes of Health Grant GM-41239 and the American Chemical Society Petroleum Research Fund Grant No. 34691-AC4. S.C.W. is a Fellow of the American Foundation for Pharmaceutical Education.

* Address correspondence to this author. Tel: (512)-471-6198. Fax: (512)-232-2606. E-mail: whitman@mail.utexas.edu.

§ The University of Texas.

‡ MRC Centre for Protein Engineering.

[1] Abbreviations: BCA, bicinchoninic acid; CHMI, 5-(carboxymethyl)-2-hydroxymuconate isomerase; COHED, 5-(carboxymethyl)-2-oxo-3-hexene-1,6-dioate decarboxylase; DEAE, diethylaminoethyl; FAH, fumarylacetoacetate hydrolase; HPLC, high-pressure liquid chromatography; IPTG, isopropyl β-D-thiogalactoside; NMR, nuclear magnetic resonance; 4-OT, 4-oxalocrotonate tautomerase; 4-OD, 4-oxalocrotonate decarboxylase; SDS−PAGE, sodium dodecyl sulfate−polyacrylamide gel electrophoresis; THF, tetrahydrofuran; TLC, thin-layer chromatography; VPH, vinylpyruvate hydratase.

10.1021/bi049489p CCC: $27.50
Published on Web 07/21/2004

Scheme 3

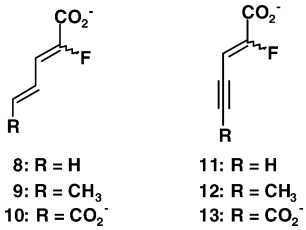

4-OT processes both mono- and dicarboxylated dienols but with different reactivities and stereochemical consequences. The 4-OT-catalyzed conversion of **1** to **5** is rapid ($k_{cat}/K_m \approx 10^7$ M^{-1} s^{-1}), while that of **2** to **4** is much slower ($k_{cat}/K_m \approx 10^2$ M^{-1} s^{-1}) (*5*,*8*). Moreover, in D_2O, 4-OT converts **1** to [5-D]**5** in D_2O in a highly stereoselective fashion, resulting in primarily the 5*S* isomer (*8*). In contrast, the enzymatic conversion of **2** to [3-D]**4** generates a mixture of isomers with the 3*R* isomer being the predominant one (*5*). While the structural basis for these observations is not known, it may reflect different binding modes for the mono- and dicarboxylated compounds. To set the stage for a crystallographic analysis to answer this question, the 2-fluoro analogues of **1** and **2** were synthesized and evaluated as potential competitive inhibitors of 4-OT. In addition, these compounds would be useful probes for crystallographic analyses of VPH as well as several recently discovered 4-OT homologues, which also process dienol substrates (*9*). As a result of our efforts to generate a 4-OD/VPH complex containing only the hydratase activity for these studies, we identified 4-OD as a member of the fumarylacetoacetate hydrolase (FAH) superfamily.

The synthesis and evaluation of these analogues are reported herein. Compounds **8**, **9**, and **10** (Scheme 3) are the 2-fluoro analogues of **1** and **2**, while compounds **11**, **12**, and **13** (Scheme 3) are the 2-fluoro-4-alkyne derivatives. The alkene derivatives are accurate mimics of the dienol substrates, while the alkyne derivatives are more rigid compounds with shortened bond lengths, which may provide additional insights due to a reduction in the degrees of freedom. Both the 2*E* and 2*Z* isomers of **8** and 4*E*-**9** were obtained, while 4*E*-**10** was obtained as a mixture of isomers with the 2*E*, 4*E* isomer being predominant. In the second series of compounds, both the 2*E* and 2*Z* isomers of **11** were obtained, while only 2*E*-**12** and 2*Z*-**13** were obtained. The compounds were evaluated as potential reversible inhibitors of 4-OT, YwhB, a closely related 4-OT homologue from *Bacillus subtilis* (*9*), and VPH in the E109Q-4-OD/VPH complex. All were found to be potent competitive inhibitors of 4-OT with K_i values ranging from 110 nM (2*E*-**8**) to 50 μM (2*Z*-**11**). The compounds were also competitive inhibitors of YwhB but with considerably higher K_i values (160−985 μM). Only the 2*E* and 2*Z* isomers of **11** were found to competitively inhibit VPH. The potencies and the competitive nature of these inhibitors suggest that they will be useful ligands in crystallographic studies of the respective enzymes. Analysis of the resulting structures will provide a structural basis for the observed inhibition and, by inference, further insights into substrate binding and catalysis. These compounds may also have general utility as inhibitors for the study of other enzymes that degrade aromatic or haloaromatic hydrocarbons, as well as 4-OT and VPH homologues.

EXPERIMENTAL PROCEDURES

Materials. All reagents, enzymes, buffers, and solvents were obtained from Sigma Aldrich Chemical Co. (St. Louis, MO), unless noted otherwise. The synthesis of 2-hydroxy-2,4-hexadienedioate (**1**) and 2-hydroxy-2,4-pentadienoate (**2**) are described elsewhere (*4*,*6*). 4-OT and YwhB were expressed in *Escherichia coli* strain BL21-Gold(DE3)pLysS (Stratagene, La Jolla, CA) and purified according to previously published procedures (*10*). The yields of 4-OT and YwhB were ~40 mg per liter of bacterial culture. Bacterial culture media, PCR reagents, molecular biology kits and reagents, oligonucleotide primers, and the bacterial strains used for the construction of the 4-OD mutants were obtained from sources listed elsewhere (*6*).

General Methods. Techniques for restriction digestions, ligations, plasmid purification, and other standard molecular biology manipulations were based on methods described elsewhere (*11*). DNA sequencing was performed at the DNA Core Facility in the Institute for Cellular and Molecular Biology at the University of Texas (Austin, TX). Protein concentrations were determined using the commercially available bicinchoninic acid (BCA) protein assay kit or the method of Waddell (*12*). High-performance liquid chromatography (HPLC) was performed on a Beckman System Gold HPLC (Fullerton, CA) using TSKgel Phenyl-5PW hydrophobic and TSKgel DEAE-5PW anion-exchange columns (Tosoh Bioscience, Montgomeryville, PA). Protein was analyzed by Tris−glycine sodium dodecyl sulfate−polyacrylamide gel electrophoresis (SDS−PAGE) under denaturing conditions on 17.5% gels using a vertical gel electrophoresis apparatus obtained from Bio-Rad (Hercules, CA) (*13*). Kinetic data were obtained using a Hewlett-Packard 8452A or an Agilent 8453 diode array spectrophotometer. NMR spectra were obtained on a Bruker AM-250 spectrometer or a Bruker AM-500 spectrometer as indicated. Chemical shifts were referenced as noted below.

Sequence Analyses. An iterative PSI−BLAST search of the NCBI nonredundant database was performed using the amino acid sequence of 4-OD (GI, 486748) from the TOL plasmid pWW0 of *Pseudomonas putida* mt-2 as the query sequence (*14*). The databases were searched with the "NR" option (all nonredundant GenBank CDS translations + PDB + SwissProt + PIR + PRF). One iteration of PSI−BLAST resulted in more than 50 sequences judged to be homologues based on significance scores. These sequences included 4-OD and VPH homologues. After removing the sequences corresponding to VPH and the 4-OD redundancies, we subjected the 19 remaining sequences to multiple-sequence alignment analysis using version 1.82 of the CLUSTAL W multiple-sequence alignment routines in the computational tools at the EMBL Web site (*15*).

Similarly, two iterative PSI−BLAST searches of the NCBI nonredundant database were performed using the amino acid sequence of YcgM (GI, 26247493), a putative isomerase from *E. coli* as the query sequence (*14*). These searches identified over 400 protein sequences judged to be homologues based on significance scores. Among these were 17 amino acid sequences corresponding to 4-ODs from various prokaryotic species. 4-OD from *P. putida* HS12 (GI, 13446765) was used to identify additional homologous sequences in a new PSI−BLAST search. One iteration of

PSI−BLAST with the new search sequence identified more than 160 additional homologous proteins, including that of 4-OD encoded by the TOL plasmid pWW0. Sequence alignment of YcgM (residues 53−212) with 4-OD from *P. putida* HS12 (residues 83−243) and a sequence alignment of 4-OD from *P. putida* HS12 (residues 83−243) with 4-OD encoded by the TOL plasmid (residues 91−254) enabled the manual alignment of YcgM with 4-OD encoded by the TOL plasmid (as shown in Figure 2).

Construction of the E109Q- and E111Q-4-OD/VPH Mutant Enzymes. The E109Q and E111Q mutants of 4-OD were constructed by overlap extension PCR (*16*). The external primers were oligonucleotides 5′-TAATACGACTCACTATAGG-3′ (designated primer A) and 5′-GCTAGTTATTGCTCAGCGG-3′ (designated primer D). Primer A corresponds to the coding sequence of the T7 promoter region of the pET-24a(+) vector, while primer D corresponds to the complementary sequence of the region upstream from the T7 terminator region of the vector. For the E109Q mutant, the internal primers were 5′-GATTTCCGCCTGGATCTTCG-3′ (primer B) and 5′-CGAAGATCCAGGCGGAAATC −3′ (primer C). For the E111Q mutant, the internal primers were 5′-GACCACCGCTATTTGTGCCTCGAT-3′ (primer B) and 5′-ATCGAGGCACAAATAGCGGTGGTC −3′ (primer C). The mutations are underlined and the remaining bases correspond to the coding sequence (primer C) or the complementary sequence (primer B) for the gene encoding 4-OD. For the E111Q mutant, silent mutations were introduced to eliminate secondary structure formation in the primers.

The PCR was carried out in a Perkin-Elmer DNA thermocycler 480 using template DNA, synthetic primers, *Taq* polymerase, and the PCR reagents following a previously described protocol (*6*, *17*). The AB and CD fragments were synthesized in separate PCRs using pET-24a-4-OD/VPH (0.7 μg) as template. For the E109Q mutant, the PCR consisted of 25 cycles, a 2-min incubation period at 94 °C preceding the 25 cycles, and a 5-min incubation period at 72 °C following the 25 cycles. Each cycle consisted of three steps: denaturation at 94 °C for 1 min, annealing at 55 °C for 1.25 min, and elongation at 72 °C for 1.25 min. For the E111Q mutant, the PCR also consisted of 25 cycles but had a 1-min incubation period at 94 °C preceding the 25 cycles and the 5-min incubation period at 72 °C following the 25 cycles. Each cycle of the E111Q mutant protocol consisted of three steps: denaturation at 94 °C for 0.75 min, annealing at 55 °C for 0.75 min, and elongation at 72 °C for 3.5 min. The amplification products were analyzed and purified as described (*6*, *17*). The AD segment was constructed similarly using the AB and CD fragments as template (1 μL each) and the conditions described above. The resulting mutated DNA fragment and the pET-24a(+) vector were treated with *Xba*I and *Hind*III restriction enzymes, purified, and ligated using T4 DNA ligase as described (*6*, *17*). The DNA was precipitated, resuspended in 10 μL of sterile water, and transformed into *E. coli* DH5α cells by electroporation, and the transformed cells were grown overnight at 37 °C on LB/Kn (100 μg/mL) plates. For the E109Q mutant, 20 randomly selected colonies were screened for the plasmid insert using methods described elsewhere (*17*). For the E111Q mutant, 12 randomly selected colonies were similarly screened for insert (*17*). Colonies containing the appropriate plasmids were grown in liquid LB/Kn (10 mL, 100 μg/mL) medium at 37 °C overnight, and the newly constructed plasmids (designated pET-24a−E109Q4-OD/VPH or pET-24a−E111Q4-OD/VPH) were isolated using the Wizard Miniprep kit (Promega, Madison, WI) according to the manufacturer's instructions. The mutations were confirmed by DNA sequence analysis. The plasmids were individually introduced into *E. coli* strain BL21(DE3)pLysS by electroporation as described (*17*).

Expression and Purification of the E109Q- and E111Q-4OD/VPH Mutants. The two 4-OD mutants were expressed and purified according to a modification of previously published procedures (*2*,*6*). Accordingly, cultures were induced using isopropyl β-D-thiogalactoside (IPTG) (0.5 mM) at an OD_{600} reading of ∼0.6−0.8 and grown for 4 h postinduction before harvesting. Under these conditions, 1.5 L of bacterial culture yields 3 g of cells, which were stored at −80 °C until use. The cells were resuspended in a volume (3 × cell weight) of 10 mM ethylenediamine buffer (pH 7.3) containing 10% 2-propanol (designated buffer A) and made 5 mM in $MgCl_2$. The suspension was initially disrupted by sonication (50% output) for 30 s. After the mixture was made 0.5 mM in phenylmethylsulfonyl fluoride and 1 mM in 6-aminocaproic acid, it was further sonicated for 3 5-min intervals using 5-s pulses with 50% cycle time. Each 5-min sonication interval was separated by a 5-min resting period.

After centrifugation (19 000 rpm, 30 min), the supernatant was made 1.2 M in $(NH_4)_2SO_4$ and stirred for 1 h at 4 °C. The resulting solution was centrifuged (17 000 rpm, 30 min), and the supernatant was loaded onto a Phenyl-5PW column (1.5 cm × 21.5 cm), which had been equilibrated in 10 mM ethylenediamine buffer (pH 7.3) made 1.2 M in $(NH_4)_2SO_4$ (designated buffer B), attached to the Beckman System Gold HPLC. The protein was eluted using a 10-min wash of 100% buffer B, a 50-min linear gradient from 100% buffer B to 100% buffer A, and a final 10-min wash of 100% buffer A. The flow rate was 5 mL/min. Fractions (7.5 mL) were collected and assayed for activity. Typically, the mutants elute at ∼0.15 M $(NH_4)_2SO_4$. The most active fractions were pooled, concentrated, and exchanged (85−90%) into 20 mM Tris-HCl buffer, pH 7.3 (designated buffer C), using an Amicon stirred cell equipped with a YM-10 membrane.

The resulting concentrate was loaded onto a DEAE-5PW column equilibrated in buffer C. The protein was eluted using a 10-min wash of 100% buffer C, followed by a 60-min linear gradient of buffer C containing NaCl (0−0.4 M) at a flow rate of 5 mL/min. Fractions (7.5 mL) were collected and assayed for activity. The mutants elute at ∼0.25 M NaCl. The most active fractions were pooled, concentrated, and made ∼2 mM in $MgCl_2$. The yield of E109Q4-OD/VPH (∼95% pure by SDS−PAGE) is approximately 15 mg per liter of bacterial culture. The yield of E111Q4-OD/VPH (∼95% pure by SDS−PAGE) is approximately 14 mg per liter of bacterial culture.

*Syntheses of the 2E and 2Z Isomers of 2-Fluoro-2,4-pentadienoic Acid (**8**).* To a stirring solution of triethyl 2-fluoro-2-phosphonoacetate (**14**, 1 g, 4.1 mmol) in 20 mL of anhydrous toluene at −78 °C was added 1 equiv of *tert*-butyllithium (1.7 M in pentane) dropwise over a 5 min period (*18*). After the solution was stirred for 1 h under argon at −78 °C, freshly distilled acrolein (**15**, 1 mL, 15 mmol) was rapidly added. The solution continued to stir under argon

and was allowed to come to room temperature overnight. Subsequently, the reaction mixture was concentrated, placed on a flash column, and eluted with toluene to result in a partial separation of the 2*E* and 2*Z* isomers with the 2*E* isomer predominating. Fractions containing the 2*E* isomer were combined and incubated with I_2 (100 mg, 0.4 mmol) overnight. The solution was washed with 5% sodium bisulfite, dried over anhydrous $MgSO_4$, and subjected to flash chromatography. After elution with toluene, fractions containing the 2*Z* isomer of ethyl 2-fluoro-2,4-pentadienoate (**18**) were combined. The volatility of **18** coupled with the presence of toluene precluded its isolation and NMR characterization. Hence, **18** was processed without further purification. Accordingly, ethanol (20 mL) and an aqueous solution of 2 M NaOH (50 mL) were added to the combined fractions. After the mixture was stirred overnight at room temperature, most of the solvent was removed, and the residue was diluted with water (100 mL). The pH was adjusted to ~2 using H_2SO_4. The resulting mixture was extracted with ethyl acetate (3 × 100 mL), and the organic layers were collected and dried over anhydrous Na_2SO_4. The solvent was removed to yield 2*Z*-**8** as a pale yellow solid (58 mg). 2*Z*-**8**: ^{1}H NMR (CD_3OD, 500 MHz) δ 5.44 (1H, dt, J = 10 Hz, $H5_{cis}$), 5.62 (1H, dt, J = 16 Hz, $H5_{trans}$), 6.64 (1H, dd, J_{HF} = 37 Hz, H3), 6.67 (1H, m, H4); ^{13}C NMR (CD_3OD, 62 MHz) δ 119.4, 119.5 (d, C3), 124.9, 125.0 (d, C4), 128.4 (d, C5), 146.2, 150.4 (d, $J_{C,F}$ = 262 Hz, C2), 163.4, 164.0 (d, C1); ^{19}F NMR (CD_3OD, 469.8 MHz) δ −129.22, −129.16 (d, 1F, $^3J_{FH}$ = 32 Hz).

The fractions containing the ethyl ester of largely the 2*E* isomer were hydrolyzed similarly to yield 2*E*-**8** (640 mg). 2*E*-**8**: ^{1}H NMR (CD_3OD, 250 MHz) δ 5.39 (1H, d, J = 10 Hz, $H5_{cis}$), 5.52 (1H, d, J = 17.1 Hz, $H5_{trans}$), 6.50 (1H, dd, J_{HF} = 19.8 Hz, H3), 7.25 (1H, dt, H4); ^{13}C NMR (CD_3OD, 62 MHz) δ 122.9, 123.3 (d, C3), 124.6, 124.7 (d, C4), 131.2, 131.3 (d, C5), 146.7, 150.8 (d, $J_{C,F}$ = 255 Hz, C2), 165.9, 168.2 (d, C1); ^{19}F NMR (CD_3OD, 469.8 MHz) δ −123.05, −123.01 (d, 1F, $^3J_{FH}$ = 20 Hz).

*Syntheses of the 2E and 2Z Isomers of Ethyl 2-Fluoro-2,4E-hexadienoate (**19**) and Diethyl 2-Fluoro-4E-hexadienedioate (**20**).* To a stirring solution of triethyl 2-fluoro-2-phosphonoacetate (**14**, 1.5 g, 6.2 mmol) in 30 mL of anhydrous THF at −78 °C was added 1 equiv of *tert*-butyllithium (1.7 M in THF) dropwise over a 5 min period (*18*). After the mixture was stirred for 1 h under argon, 1.1 equiv of the aldehyde (**16** or **17**) dissolved in 5 mL of THF was rapidly added. Aldehyde **17** was synthesized by a literature procedure using SeO_2 (*19*). The solution continued to stir under argon and was allowed to warm to room temperature overnight. Subsequently, it was concentrated under reduced pressure to remove most of the THF. The crude products were purified by flash chromatography (9:1 hexanes/ethyl acetate) to give **19** (1.86 g using 4.8 g of **14**, 59%) and **20** (1.18 g, 88%) as oils. The 2*E* and 2*Z* isomers of **19** can be nearly completely separated by flash chromatography (as estimated by ^{1}H NMR spectroscopy) using toluene as the eluant. 2*E*,4*E*-**19**: ^{1}H NMR ($CDCl_3$, 250 MHz) δ 1.32 (3H, t, CH_3 of OCH_2CH_3), 1.79 (3H, dt, H6), 4.29 (2H, t, CH_2 of OCH_2CH_3), 6.08 (1H, q, H5), 6.48 (1H, dd, J_{HF} = 20.2 Hz, H3), 6.94 (1H, t of t, H4); ^{13}C NMR (CD_3OD, 62 MHz) δ 14.4 (CH_3 of OCH_2CH_3), 18.9 (C6), 62.4 (CH_2 of OCH_2CH_3), 123.6, 124.0 (d, C3), 125.4 (d, C4), 139.8 (C5), 144.3, 148.3 (d, $J_{C,F}$ = 253 Hz, C2), 162.0, 162.6 (d, C1).

The 2*E*,4*E*-isomer of **20** is the predominant product of the reaction between **14** and **17**, but a small amount (~10%) of the 2*Z*,4*E*-isomer is present as determined by ^{1}H NMR spectroscopy. 2*E*,4*E*-**20**: ^{1}H NMR ($CDCl_3$, 250 MHz) δ 1.20, (3H, t, CH_3 of OCH_2CH_3), 1.30 (3H, t, CH_3 of OCH_2CH_3), 4.15 (2H, q, CH_2 of OCH_2CH_3), 4.30 (2H, q, CH_2 of OCH_2CH_3), 6.05 (1H, d, J = 15.6 Hz, H5), 6.45 (1H, dd, H3), 8.10 (1H, dd, H4); ^{13}C NMR (CD_3Cl, 62 MHz) δ 13.8, 14.0 (CH_3 of OCH_2CH_3), 60.5, 62.0 (CH_2 of OCH_2CH_3), 118.5, 118.9 (d, C3), 127.6, 127.8 (d, C5), 136.1, 136.2 (d, C4), 148.2, 152.5 (d, $J_{C,F}$ = 270 Hz, C2), 159.4, 160.0 (d, C1), 165.5 (C6).

*Syntheses of the 2E and 2Z Isomers of 2-Fluoro-4E-hexadienoic Acid (**9**) and 2-Fluoro-4E-hexadienedioic Acid (**10**).* The hydrolysis of **19** or **20** was carried out by suspending the individual compounds in a chilled (0 °C) solution of 1 M NaOH (30 mL). After allowing the solution to warm to room-temperature overnight, we adjusted the pH to ~2 using a solution of 8.5% phosphoric acid. The resulting mixture was extracted with ethyl acetate (3 × 200 mL), and the organic layers were collected and dried over anhydrous Na_2SO_4. The solvent was removed, and the residue was crystallized from a solution of ethyl acetate and benzene. The yields were 26 mg for the 2*E*-isomer and 680 mg for the 2*Z*-isomer. 2*E*,4*E*-**9**: ^{1}H NMR ($CDCl_3$, 250 MHz) δ 1.85, (3H, dt, H6), 6.07 (1H, q, J = 14.7 Hz, H5), 6.52 (1H, dd, J_{HF} =19.5 Hz, H3), 6.93 (1H, dt, H4); ^{19}F NMR ($CDCl_3$, 469.8 MHz) δ −127.73, −127.77 (d, 1F, $^3J_{FH}$ = 17.4 Hz). 2*Z*,4*E*-**9**: ^{1}H NMR (CD_3OD, 250 MHz) δ 1.84, (3H, dt, H6), 6.15 (1H, q, J = 15 Hz, H5), 6.38 (1H, dt, H4), 6.60 (1H, dd, J_{HF} =31.5 Hz, H3); ^{13}C NMR (CD_3OD, 62 MHz) δ 18.9 (C6), 119.8, 120.0 (d, C3), 123.1 (C4), 139.0 (C5), 144.5, 148.6 (d, $J_{C,F}$ = 258 Hz, C2), 163.9, 164.4 (d, C1); ^{19}F NMR (CD_3OD, 469.8 MHz) δ −132.57, −132.64 (d, 1F, $^3J_{FH}$ = 29 Hz).

The hydrolysis of **20** and subsequent crystallization generated two mixtures of **10**. One mixture had an *E*/*Z* ratio of 14:1 (410 mg), and the second mixture had an *E*/*Z* ratio of 8:1 (100 mg). The *E* to *Z* ratios were estimated by ^{1}H NMR spectroscopy. 2*E*,4*E*-**10**: ^{1}H NMR ($CDCl_3$, 250 MHz) δ 6.04 (1H, d, J = 15.5 Hz, H5), 6.42 (1H, dd, J_{HF} = 17.8 Hz, H3), 8.05 (1H, dd, H4); ^{13}C NMR (acetone-d_6, 62 MHz) δ 119.6, 120.0 (d, C3), 128.8, 129.0 (d, C5), 137.7, 137.8 (d, C4), 149.5, 153.7 (d, $J_{C,F}$ = 264 Hz, C2), 167 (C1), 169.5 (C6); ^{19}F NMR (CD_3OD, 469.8 MHz) δ −112.69, −112.73 (d, 1F, $^3J_{FH}$ = 18 Hz). 2*Z*,4*E*-**10**: ^{1}H NMR ($CDCl_3$, 250 MHz) δ 6.10 (1H, d, J = 15.5 Hz, H5), 6.60 (1H, dd, J_{HF} = 28.6 Hz, H3), 7.50 (1H, dd, H4); ^{19}F NMR (CD_3OD, 469.8 MHz) δ −120.92, −120.98 (d, 1F, $^3J_{FH}$ = 30 Hz).

*Syntheses of Ethyl 2E- and 2Z-Fluoropent-2-en-4-ynoate (**24**).* In a typical procedure, 1 equiv of *tert*-butyllithium (1.7 M in pentane) was added dropwise over a 15 min period to a stirring solution of **14** (2.5 g, 10.3 mmol) in 100 mL of anhydrous THF at −78 °C. After the mixture stirred for 45 min under argon, 2-propynal (**21**, 1 g, 18.5 mmol), synthesized by a literature procedure (*20*), was added neat over 5 min. The resulting solution continued to stir under argon and was allowed to warm to room temperature overnight. Subsequently, it was concentrated under reduced pressure to remove most of the THF. The crude product was purified

by flash chromatography (toluene) to give two spots (on TLC) corresponding to the 2*E* and 2*Z* isomers. The 2*E* isomer is the predominant isomer. To maximize the yields, the appropriate fractions were combined and hydrolyzed (to 2*E*- and 2*Z*-**11**) without further purification. The yields were significantly diminished by concentration under reduced pressure due to the presence of toluene and the volatility of the compound. Nonetheless, a small portion of the fractions containing the 2*E* isomer was concentrated under reduced pressure to obtain the ^{1}H and ^{13}C NMR spectra. The low yield of the 2*Z* isomer precluded its isolation and NMR characterization. (2*E*)-**24**: ^{1}H NMR ($CDCl_3$, 250 MHz) δ 1.28 (3H, t, CH_3 of OCH_2CH_3), 3.44 (1H, dt, H5), 4.27 (2H, q, CH_2 of OCH_2CH_3), 5.91 (1H, dd, $J_{HF} = 14$ Hz, H3); ^{13}C NMR ($CDCl_3$, 62 MHz) δ 13.8 (s, CH_3 of OCH_2CH_3), 62.0 (s, CH_2 of OCH_2CH_3), 88.6, 88.8 (d, C3), 100.5, 101.4 (d, C2), 154.4, 158.5 (d, C1).

*Syntheses of Ethyl 2E-Fluorohexen-4-ynoate (**25**).* In a typical procedure, 1 equiv of *tert*-butyllithium (1.7 M in pentane) was added dropwise over a 15 min period to a stirring solution of **14** (1.5 g, 6.2 mmol) in 30 mL of anhydrous THF at −78 °C. After the mixture stirred for 45 min under argon, 2-butynal (**22**, 1 g, 14.7 mmol) was added neat over 5 min. After treating the mixture as described above, we purified 2*E*-**25** by flash chromatography (8:1 hexanes/ethyl acetate). To maximize the yield, the fractions were not evaporated to dryness. 2-Butynal was synthesized by the oxidation of the commercially available 2-butyn-1-ol using a procedure described elsewhere (*18*). The product, **22**, was isolated by fractional distillation under vacuum. (2*E*)-**25**: ^{1}H NMR ($CDCl_3$, 250 MHz) δ 1.30 (3H, t, CH_3 of OCH_2CH_3), 2.00 (3H, q, H5), 4.25 (2H, q, CH_2 of OCH_2CH_3), 5.93 (1H, dq, $J_{HF} = 14.5$ Hz, H3); ^{13}C NMR ($CDCl_3$, 62 MHz) δ 4.75 (s, C6), 13.8 (s, CH_3 of OCH_2CH_3), 61.5 (s, CH_2 of OCH_2CH_3), 71.7, 71.9 (d, C5), 98.7, 98.9 (d, C3), 102.6, 103.1, (d, C2), 152.6, 156.8 (d, C1), 159.0, 159.5 (d, C4).

*Syntheses of Diethyl 2E- and Diethyl 2Z-Fluorohex-2-en-4-yndioate (**26**).* The two isomers of **26** (with the 2*E* isomer predominating) were synthesized following the procedure described for the syntheses of 2*E*- and 2*Z*-**24** with the following modifications. The aldehyde, ethyl 3-formylprop-2-ynoate (**23**), was synthesized according to a literature procedure and generated from the diethyl acetal by treatment in concentrated HCO_2H at 80 °C for 3 h (*21*). The formic acid was removed under reduced pressure to yield crude **23** (*21*). Subsequently, **23 (**0.7 g, 5.6 mmol**)** was dissolved in anhydrous THF (5 mL) and added rapidly to the stirring solution of **14** (1.1 mL, 5.6 mmol) in 30 mL of anhydrous THF at −78 °C. After the mixture was stirred at −78 °C for 3 h under argon, a quantity (30 mL) of 100 mM NaH_2PO_4 buffer (pH ≈ 5) was added, and the resulting mixture was extracted with ethyl acetate (3 × 30 mL). The organic layers were combined, dried over anhydrous $MgSO_4$, filtered, and evaporated to dryness. The residue (containing both isomers) was initially purified using flash chromatography (8:1 hexanes/ethyl acetate). Fractions containing the two isomers were combined and evaporated to dryness. Subsequently, the isomers were separated by flash chromatography using 4:1 toluene/hexanes. This solvent system resulted in two spots (on TLC) corresponding to the 2*E* (with a lower R_f value) or the 2*Z* (with a higher R_f value) isomer. The appropriate fractions were combined and evaporated to dryness to yield predominantly the 2*E*-**26** (0.33 g, 27%) and 2*Z*-**26** (30 mg, 3%). (2*E*)-**26**: ^{1}H NMR ($CDCl_3$, 500 MHz) δ 1.30 (3H, t, CH_3 of OCH_2CH_3), 1.37 (3H, t, CH_3 of OCH_2CH_3), 4.25 (2H, q, CH_2 of OCH_2CH_3), 4.35 (2H, q, CH_2 of OCH_2CH_3), 6.02 (1H, d, $J_{HF} = 12.6$ Hz, H3); ^{13}C NMR ($CDCl_3$, 125 MHz) δ 13.8, 14.0 (s, CH_3 of OCH_2CH_3), 62.3, 62.7 (s, CH_2 of OCH_2CH_3), 77.2, 77.3 (d, C5), 89.8, 89.9 (d, C2), 98.7, 99.0 (d, C3), 153.2, 155.3, (d, C1), 158.2, 158.5 (d, C4), 159.4 (s, C6); ^{19}F NMR ($CDCl_3$, 469.8 MHz) δ −105.685, −105.659 (d, 1F, $^{3}J_{F,H} = 12$ Hz). (2*Z*)-**26**: ^{1}H NMR ($CDCl_3$, 250 MHz) δ 6.19 (1H, d, $J_{HF} = 27.8$ Hz, H3); ^{13}C NMR ($CDCl_3$, 125 MHz) δ 13.98, 14.02 (s, CH_3 of OCH_2CH_3), 62.5, 62.8 (s, CH_2 of OCH_2CH_3), 75.8, (s, C5), 90.88, 90.93 (d, C2), 96.9, 97.0 (d, C3), 153.0, 156.2, (d, C1), 159.0, 159.2 (d, C4), 161.6 (s, C6); ^{19}F NMR ($CDCl_3$, 469.8 MHz) δ −105.834, −105.775 (d, 1F, $^{3}J_{F,H} = 27.8$ Hz).

*Syntheses of 2E- and 2Z-Fluoropent-2-en-4-ynoic Acid (**11**).* The hydrolyses of 2*E*- and 2*Z*-**24** was carried out by adding 50 mL of a 2 M solution of aqueous NaOH to the fractions containing the appropriate esters as described above. In addition, ethanol (∼10 mL) was added, and the mixture was vigorously stirred such that cloudiness resulted in the toluene layer. After the mixture was stirred at room-temperature overnight, the toluene was removed under reduced pressure and the pH of the liquid residue was adjusted to ∼2 using a solution of 8.5% phosphoric acid. The resulting mixture was extracted with ethyl acetate (3 × 50 mL), and the organic layers were collected and dried over anhydrous Na_2SO_4. The solvent was removed to afford 2*E*-**11** (0.68 g) and 2*Z*-**11** (25 mg) as yellow solids. (2*E*)-**11**: ^{1}H NMR (CD_3OD, 250 MHz) δ 3.93 (1H, dd, H5), 6.14 (1H, dd, $J_{HF} = 14.7$ Hz, H3); ^{13}C NMR (CD_3OD, 62 MHz) δ 76.1, 76.4 (d, C5), 90.4, 90.6 (d, C3), 101.5, 102.1 (d, C2), 156.3, 161.3 (d, C1); ^{19}F NMR ($CDCl_3$, 469.8 MHz) δ −114.5 (dd, 1F, $^{3}J_{F,H} = 14.6$ Hz). (2*Z*)-**11**: ^{1}H NMR ($CDCl_3$, 250 MHz) δ 3.59 (1H, dd, H5), 6.25 (1H, dd, $J_{HF} = 28$ Hz, H3); ^{13}C NMR ($CDCl_3$, 125 MHz) δ 73.9 (d, C5), 91.6, 91.7 (d, C3), 101.5, 100.6 (d, C2), 153.7, 155.9 (d, C1), 163.8, 164.1 (d, C4); ^{19}F NMR ($CDCl_3$, 469.8 MHz) δ −113.6 (dd, 1F, $^{3}J_{F,H} = 28$ Hz).

*Synthesis of 2-Fluorohex-2E-en-4-ynoic Acid (**12**).* The hydrolysis of (2*E*)-**25** was carried out by suspending the compound in water (25 mL), chilling the suspension to 0 °C, and adding 1 equiv of a 0.5 M solution of aqueous NaOH over 1.5 h. After the mixture was stirred at room temperature for an additional hour, the pH of the solution was adjusted to ∼8 using a solution of 8.5% phosphoric acid. After extracting the aqueous solution with ethyl acetate to remove any remaining ester, we adjusted the pH of the aqueous solution to ∼2 using a solution of 8.5% phosphoric acid. The resulting mixture was extracted with ethyl acetate (3 × 50 mL), and the organic layers were collected and dried over anhydrous Na_2SO_4. The solvent was removed to yield 2*E*-**12** (360 mg) as an off-white solid. (2*E*)-**12**: ^{1}H NMR (CD_3OD, 500 MHz) δ 2.00 (3H, q, H6), 6.08 (1H, dq, $J_{HF} = 15$ Hz, H3); ^{13}C NMR (CD_3OD, 62 MHz) δ 4.47 (s, C6), 72.7, 72.9 (d, C5), 99.6, 99.8 (d, C3), 103.5, 104.1 (d, C2), 154.6, 158.7 (d, C1), 161.9, 162.4 (d, C4); ^{19}F NMR (CD_3OD, 469.8 MHz) δ −119.2 (d, 1F, $^{3}J_{F,H} = 14.8$ Hz).

*Synthesis of 2-Fluorohex-2Z-en-4-yndioic Acid (**13**).* The 2*Z* isomer of **26** (30 mg, 0.14 mmol) was suspended in H_2O

Scheme 4

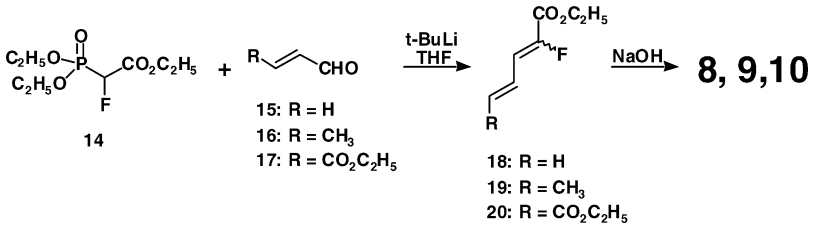

(5 mL) and chilled to 6 °C. An aqueous solution of chilled 1 M NaOH (0.35 mL) was added in one aliquot. After the reaction mixture was allowed to stir at 6 °C overnight, the pH was adjusted to 2 using a solution of 8.5% phosphoric acid, and the mixture was extracted with ethyl acetate (3 × 10 mL). The organic layers were combined and dried over anhydrous Na_2SO_4. The solvent was removed to yield 2*Z*-**13** (8 mg, 36%) as a yellow solid. A ^{1}H NMR did not display any signals corresponding to the 2*E*-isomer. ^{1}H NMR (CD_3OD, 500 MHz) δ 6.36 (1H, d, J_{HF} = 28 Hz, H3); ^{13}C NMR (CD_3OD, 125 MHz), δ 76.4 (s, C5), 92.0, 92.05 (d, C2), 97.4, 97.5 (d, C3), 155.5 (s, C4), 158.1, 160.3 (d, C1), 161.4, 161.7 (d, C6); ^{19}F NMR (CD_3OD, 469.8 MHz) −107.668, −107.730 (d, 1F, $^3J_{F,H}$ = 28.8 Hz). Hydrolysis of the 2*E* isomer of **26** by this procedure generated a solid that could not be identified.

Enzyme Assays. The activity of 4-OT was determined by a previously described assay using **1** (*4*), following the increase in absorbance at 236 nm due to the formation of **5**. The activity of YwhB was determined by a previously described assay using phenylpyruvate (**27**). Ketonization of **27** to generate **28** is followed by the decay at 288 nm (*22*).

27 **28**

The residual 4-OD activity in the E109Q- and E111Q-4-OD/VPH complexes was monitored by following the loss in absorbance at 236 nm, which corresponds to the decarboxylation of **5** (*6*, *7*). Substrate **5** is generated in situ by the action of 4-OT on **1** (*7*). The VPH activity in the E109Q- and E111Q-4-OD/VPH complexes was monitored by following the loss in absorbance at 265 nm, which corresponds to the hydration of **2** (*6*, *7*).

Inhibition Studies of 4-OT, YwhB, and E109Q4-OD/VPH. Stock solutions of inhibitors were made up in either ethanol (**8** and **9**) or 100 mM Na_2HPO_4 buffer, pH ∼9.2 (**10**−**13**). The addition of the inhibitor as a free acid to the buffer adjusted the pH of the aqueous stock solutions to ∼7. The concentrations of the stock solutions were as follows: **8**, 57.3 mM; **9**, 50.0 mM; **10**, 41.7 mM; **11**, 56.6 mM; **12**, 50.5 mM; and **13**, 42.2 mM.

A quantity of 4-OT (5 μL of a 2.15 mg/mL solution) was diluted into 200 mL of 20 mM NaH_2PO_4 buffer, pH 7.3, and allowed to equilibrate at 22 °C for at least 1 h before use. The enzyme stock solution was divided into 14-mL portions, and the inhibitors were added from stock solutions to give the desired final concentrations. After a 5-min incubation period, 1-mL aliquots were removed and assayed in the presence of varying concentrations of **1** (20−500 μM). The final concentrations of inhibitors used ranged from 0 to 100 μM.

A quantity of YwhB (25 μL of a 26.5 mg/mL solution) was diluted into 250 mL of 20 mM NaH_2PO_4 buffer, pH 7.3, and allowed to equilibrate at 29 °C for at least 1 h before use. The enzyme stock solution was divided into 20-mL portions, and the inhibitor was added to give the desired final concentration. After 5 min, an aliquot was removed and assayed in the presence of twelve concentrations of **27** (10−150 μM). The final concentrations of inhibitors used were as follows: **9**, 2.8−28 μM; **10**, 0−271 μM; 2*E*-**11**, 0−706 μM; 2*Z*-**11**, 0−395 μM; **12**, 0−555 μM; and 2*E*-**13**, 0−338 μM.

A quantity of the E109Q 4-OD/VPH complex (25 μL of a 2.5 mg/mL solution) was diluted into 250 mL of 20 mM NaH_2PO_4 buffer containing 5 mM $MgCl_2$, pH 7.3, and allowed to equilibrate at 29 °C for at least 1 h before use. The enzyme stock solution was divided into 20-mL portions, and the inhibitor was added to give the desired final concentration (0−300 μM). After 5 min, an aliquot was removed and assayed in the presence of 12 concentrations of **2** (3−178 μM). The final concentrations of inhibitors used ranged from 0 to 565 μM.

Data Analysis. The kinetic parameters for 4-OD, the 4-OD mutants, and VPH were fitted by nonlinear regression data analysis using the Grafit program (Erithacus Software Ltd., Staines, U.K., version 5.0). The kinetic data for the inhibition studies were fitted by nonlinear regression data analysis using the equation for competitive inhibition provided within the Grafit program.

RESULTS

*Syntheses of 2-Fluoro-2,4-pentadienoic Acid (**8**), 2-Fluoro-2,4-hexadienoic Acid (**9**), and 2-Fluoro-2,4-hexadienedioic Acid (**10**).* The syntheses of **8**, **9**, and **10** were carried out by a modification of a literature procedure and are outlined in Scheme 4 (*16*). Condensation of the commercially available triethyl 2-fluoro-2-phosphonoacetate (**14**) with acrolein (**15**), crotonaldehyde (**16**), or ethyl 4-oxo-2*E*-butenoate (**17**) results in the formation of **18**, **19**, or **20**, respectively. Compounds **15** and **16** are commercially available, while the synthesis of **17** was carried out as described elsewhere using selenium dioxide (*19*). Saponification of the esters (**18**, **19**, and **20**) followed by acidification afforded the desired compounds (**8**, **9**, and **10**) as their free acids.

*Assignment of the Configurations of **8**, **9**, and **10**.* Both the 2*E* and 2*Z* isomers of **8** and the 2*E* and 2*Z* isomers of 4*E*-**9** were generated. The individual isomers were separated by flash chromatography using toluene as the eluant. The diacid **10** was obtained as a mixture of the 2*E*,4*E* and 2*Z*,4*E* isomers with the former being predominant. In one mixture, the ratio of *E* to *Z* isomer for **10** was 8 to 1, while in a second mixture, the ratio of *E* to *Z* isomer was 14 to 1. The *E* configuration at C-4 of **9** and **10** was established by the *E*

Scheme 5

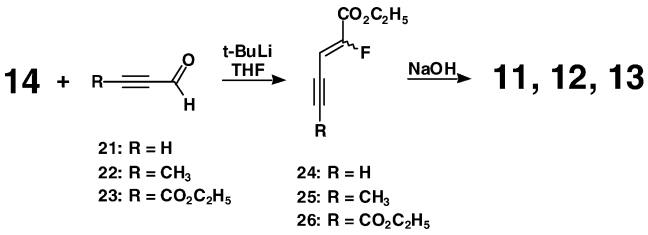

configuration of the starting materials (aldehydes **16** and **17**) for the condensation reaction and the coupling constants measured for the products **9** and **10**. Crotonaldehyde (**16**) is commercially available primarily as its *E*-isomer, while 3*E*-**17** was synthesized and used in the condensation reaction. In addition, the coupling constants for the proton at C-5 of both **9** (15 Hz) and **10** (15.5 Hz) are consistent with the *E*-configuration (*4*).

The configurations for the C-2 bonds of **8**, **9**, and **10** were determined on the basis of the vicinal H−F coupling constants observed in the ^{1}H and ^{19}F NMR spectra. In the ^{1}H NMR spectra, the 2*E* isomers (where the hydrogen and the fluoro substituent are on the same side of the double bond) have smaller H−F coupling constants (20 and 18 Hz, respectively), while the 2*Z* isomers (where the hydrogen and the fluoro substituent are on the opposite of the double bond) have larger H−F coupling constants (37 and 29 Hz, respectively). Similarly, in the ^{19}F NMR spectra (of **8** and **9**), the 2*E* isomers have smaller F−H coupling constants (20 and 17 Hz, respectively) than the 2*Z* isomers (32 and 29 Hz, respectively). These observations are consistent with those reported in the literature (*23*−*26*).

The position of the fluoro substituent also affects the chemical shifts of the protons at C-3 and C-4 of **8**, **9**, and **10**. The chemical shift for the C-3 proton in the 2*E* isomer is slightly upfield (∼0.12−0.14 ppm) from that observed for the same proton in the 2*Z* isomer. The chemical shift for the C-4 proton is more significantly upfield (0.54−0.55 ppm) in the 2*Z* isomer than for the same proton in the 2*E* isomer. In the 2*E* isomer, the fluoro substituent and proton on C-3 are on the same side of the double bond, while in the 2*Z* isomer, the fluoro substituent and the proton on C-4 are on the same side of the double bond. In both cases, the proximity of the fluoro substituent to the proton moves the signal upfield.

*Syntheses of 2-Fluoropent-2E- and 2-Fluoropent-2Z-en-4-ynoic Acid (**11**), 2-Fluorohex-2E-en-4-ynoic Acid (**12**), and 2-Fluorohex-2Z-en-4-yndioic Acid (**13**).* The syntheses of **11**, **12**, and **13** are outlined in Scheme 5. Condensation of **14** with 2-propynal (**21**), 2-butynal (**22**), or ethyl 4-oxo-2-butynoate (**23**) affords **24**, **25**, and **26**, respectively. The synthesis of **21** is described elsewhere (*20*). Aldehyde **22** was synthesized similarly by the oxidation of the commercially available 2-butyn-1-ol. The synthesis of **23** from ethyl 4,4-diethoxybut-2-ynoate has also been previously described (*21*). Saponification of the esters (**24**, **25**, and **26**) followed by acidification afforded the desired compounds (**11**, **12**, and **13**) as their free acids.

*Assignment of the Configurations of **11**, **12**, and **13**.* For compound **11**, both the 2*E* and 2*Z* isomers were generated in the synthetic reaction with the 2*E* isomer predominating. The isomers could be separated by flash chromatography using toluene as the eluant. For **12**, only the 2*E* isomer was obtained. Both 2*E*- and 2*Z*-**26**, the diethyl ester precursors for **13**, were obtained in the condensation reaction with the 2*E* isomer being the major product. However, hydrolysis of the 2*E* isomer resulted in an unidentified product. Hydrolysis of the 2*Z* isomer generated 2*Z*-**13**.

The configurations for the C-2 bonds of **11**, **12**, and **13** were determined on the basis of the vicinal H−F coupling constants observed in the ^{1}H and ^{19}F NMR spectra. In the ^{1}H NMR spectra, the 2*E* isomers of **11** and **12** (where the hydrogen and the fluoro substituent are on the same side of the double bond) have small H−F coupling constants (15 Hz), while the 2*Z* isomers of **11** and **13** (where the hydrogen and the fluoro substituent are on opposite sides of the double bond) have large H−F coupling constants (28 Hz). The coupling constants for 2*E*- and 2*Z*-**26**, observed in both the ^{1}H and ^{19}F NMR spectra, are consistent with this analysis. In addition, all of these observations are consistent with those reported above, as well as those reported in the literature (*23*−*26*).

Production, Expression, and Kinetic Evaluation of the E109Q- and E111Q-4OD/VPH Complexes. 4-OD and VPH are fully active when expressed as a complex in the presence of a divalent metal ion (Mn^{2+} or Mg^{2+}) (*2*). Expression of the individual genes results in unstable or insoluble enzyme (*2*, *6*). Hence, our strategy for the study of the individual enzymes is to express complexes in which one enzyme has been inactivated by the mutagenesis of a critical residue identified by sequence analysis. This approach successfully produced a 4-OD/E106QVPH complex that retains full 4-OD activity but is devoid of VPH activity (*6*).

To facilitate future studies of VPH, two complexes in which 4-OD is inactive but VPH is fully active were constructed. Conserved and potentially critical residues were initially identified by sequence alignment of the *P. putida* mt-2 4-OD, 13 sequences encoding known 4-ODs from various degradative pathways, and five putative 4-OD homologues (Figure 1). The sequences in the latter group (*Dechloromonas aromatica*, *Bordetella parapertussis*, *Bordetella bronchiseptica*, *Ralstonia solanacearum*, and *Myxococcus xanthus*) show 34−41% pairwise sequence identity with 4-OD encoded by the TOL plasmid pWW0 in *P. putida* mt-2. The 20 conserved residues in these sequences include four conserved aspartate residues (D-88, D-145, D-162, and D-182 using the *P. putida* mt-2 numbering system) and three conserved glutamate residues (E-109, E-111, and E-142). These seven conserved acidic residues were targeted for site-directed mutagenesis because a similar approach resulted in the successful construction of the 4-OD/E106QVPH complex (*6*).

Changing Glu-109 or Glu-111 to a glutamine (in individual mutants) and coexpression of E109Q- or E111Q-4-OD with VPH generates complexes with significantly reduced 4-OD activity but wild-type VPH activity (Table 1). DNA sequencing confirmed that no other mutations had been introduced. The E109Q-4-OD mutant shows a significant increase in K_m (∼7-fold) and a 2270-fold decrease in k_{cat} relative to wild-type. As a result, the k_{cat}/K_m value displays a 1.0×10^4-fold decrease. The E111Q-4-OD mutant has a comparable K_m to that of wild-type but shows a 3400-fold decrease in k_{cat}. The k_{cat}/K_m value reflects the difference in k_{cat}, showing a 3.0×10^3-fold decrease. The VPH activity in both mutants is

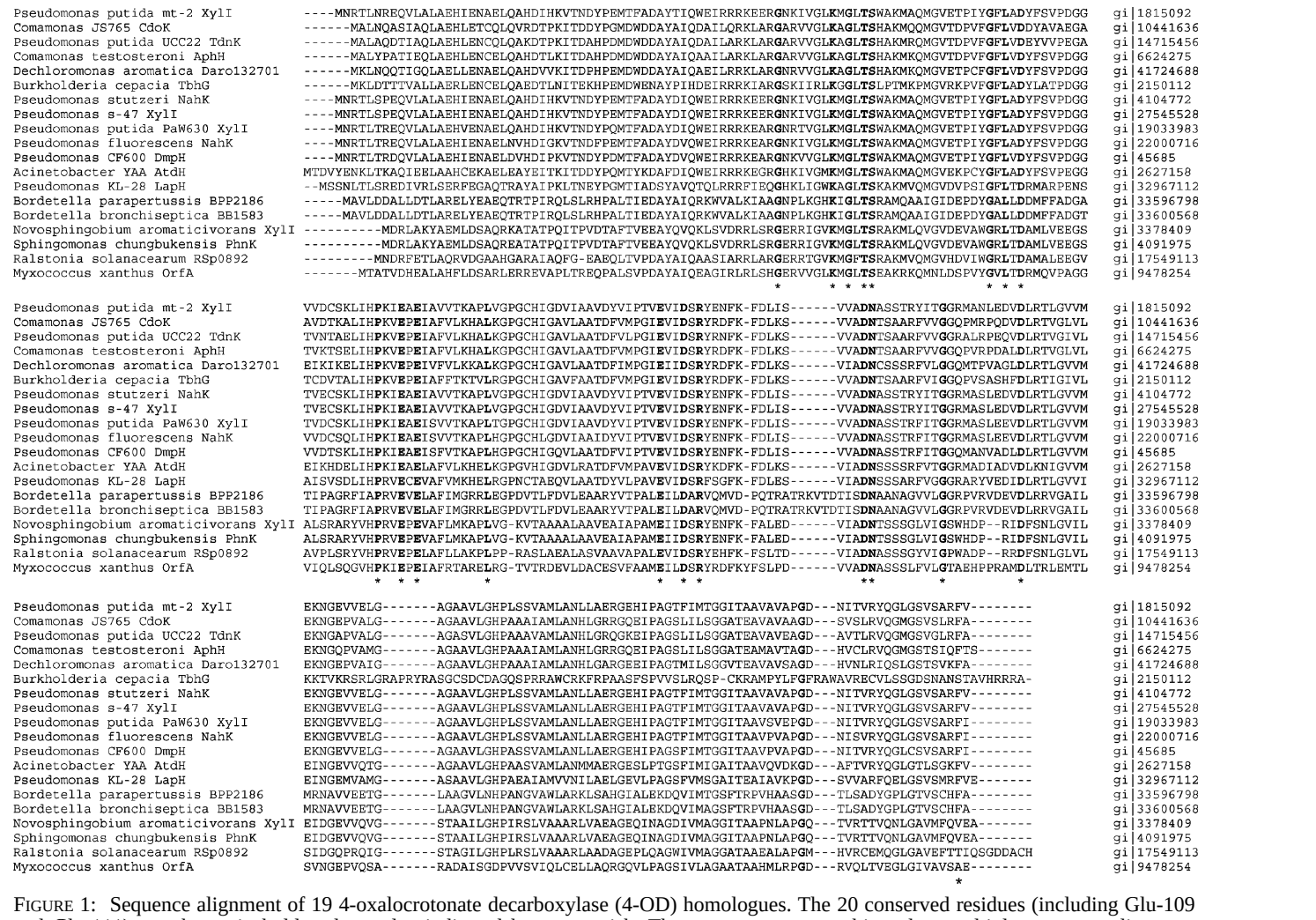

FIGURE 1: Sequence alignment of 19 4-oxalocrotonate decarboxylase (4-OD) homologues. The 20 conserved residues (including Glu-109 and Glu-111) are shown in bold and are also indicated by an asterisk. The sequences were subjected to multiple-sequence alignment analysis using version 1.82 of the CLUSTAL W multiple-sequence alignment routines in the computational tools at the EMBL Web site (*15*).

Table 1: 4-OD and VPH Activities in the E109Q- and E111Q-4-OD/VPH Complexes

enzyme	activity		
	K_m (μM)	k_{cat} (s^{-1})	k_{cat}/K_m (M^{-1} s^{-1})
4-OD Activity			
4-OD/VPH[a]	6.6 ± 0.6[b]	68 ± 2	1.0×10^7
E109Q4-OD/VPH	47 ± 7	0.030 ± 0.003	6.4×10^2
E111Q4-OD/VPH	6 ± 1	0.020 ± 0.003	3.3×10^3
VPH Activity			
4-OD/VPH	11 ± 2	360 ± 20	3.3×10^7
E109Q4-OD/VPH	11 ± 2	370 ± 14	3.4×10^7
E111Q4-OD/VPH	14 ± 2	390 ± 20	2.8×10^7

[a] The kinetic parameters for the 4-OD/VPH complex are taken from ref 6. [b] Errors are standard deviations.

comparable to that observed for the wild-type complex. Thus, the 4-OD mutations do not significantly affect the steady-state kinetic parameters of VPH. The E109Q-4-OD/VPH complex was used in the kinetic analysis due to its lower 4-OD activity (as assessed by the k_{cat}/K_m value).

Identification of 4-OD as a FAH Superfamily Member. To gain insight into the roles of these two glutamate residues, sequence analysis was carried out using the amino acid sequence of YcgM, a putative isomerase found in *E. coli*, and a member of the fumarylacetoacetate hydrolase (FAH) superfamily, the structure of which has been solved. Two PSI−BLAST iterations yielded over 400 proteins judged to be homologous. Although this list included 17 4-OD homologues, the amino acid sequence for 4-OD encoded by the TOL plasmid was not among them. One sequence, corresponding to 4-OD from *P. putida* HS12, was used to identify additional homologues in a new PSI−BLAST search. This search produced 160 additional homologues, including 4-OD encoded by the TOL plasmid, which shares 48% sequence identity with the 4-OD from *P. putida* HS12. Alignment of the two 4-OD sequences coupled with an alignment of the YcgM and *P. putida* HS12 4-OD sequences allowed the manual alignment of YcgM with 4-OD from the TOL plasmid (Figure 2). The regions shown (residues 53−212 in YcgM and residues 91−254 in 4-OD) depict the greatest sequence identity (~16%) and similarity (~54%). This analysis places 4-OD in the FAH superfamily.

The FAH superfamily consists of three structurally characterized members: YcgM; 5-(carboxymethyl)-2-oxo-3-hexene-1,6-dioate decarboxylase (COHED), which catalyzes the decarboxylation of a structurally similar substrate to that of **5** (*27*); and the mouse enzyme, fumarylacetoacetate hydrolase (FAH) (*28*). In the crystal structure of a COHED·calcium complex, three residues, Glu-276, Glu-278, and Asp-307, are coordinated to the metal ion (*29*). The two glutamate

```
YcgM : 53  LCDLRQPLAIPSDFGSVHHEVELAVLIGATLR-QATEE-HVRKAIAGYGVALDLTLRDVQG 111
4-OD : 91  SVPDGGVVDCSKLI-HPKIEAEIAVVTKAPLVGPGCHIGDVIAAVDYVIPTVEVI--DSRY 148
                  :   . . . : * *:**:  * *     .  .*  *:  .   :::   * .

YcgM : 112 KMKKAGQPWEKAKAFDNSC-PLSGFIP--AAEFTGDPQNTTLSLSVNGEQRQQGTTADMIH 169
4-OD : 149 ENFKFDLISVVADNASSTRYITGGRMANLED---VDLRTLGVVMEKNGEVVELGAGAAVLG 206
           .  *       *.  ..:    * .         * ..  : .. ***  . *  * .:

YcgM : 170 KIVPLIAYMS-----KFFTLKAGDVVLTGTPDGVGPLQSGDELTVTFD 212
4-OD : 207 HPLSSVAMLANLLAERGEHIPAGTFIMTGGITAAVAVAPGDNITVRYQ 254
           : :  :*..     :  .: **..:.** .    :  **.:**.:.
```

FIGURE 2: Amino acid sequence alignment between YcgM (residues 53−212) and 4-OD from the TOL plasmid pWW0 (residues 91−254). Residues in bold print represent the metal binding motif of YcgM (**EVE**) and the corresponding sequence of 4-OD (**EAE**). Aligned residues that are identical are marked with an ∗ beneath the sequences. Residues that are homologous with respect to hydrophobicity/hydrophilicity or charge are marked with · for lower homology, and : to depict a higher degree of homology.

Table 2: Inhibition Constants for Compounds **8**−**10** Using 4-OT and YwhB

	K_i (μM)	
inhibitor	4-OT	YwhB
2*E*-**8**	0.11 ± 0.01	
2*Z*-**8**	0.34 ± 0.04	
2*E*-**9**	2.2 ± 0.3	160 ± 20
2*Z*-**9**	8.5 ± 0.8	275 ± 54
2*E*/2*Z*-**10** (8:1)	36 ± 7	210 ± 40
2*E*/2*Z*-**10** (14:1)	45 ± 7	223 ± 40

[a] Errors are standard deviations.

Table 3: Inhibition Constants for Compounds **11**−**13** Using 4-OT, YwhB, and VPH

	K_i (μM)		
inhibitor	4-OT	YwhB	VPH
2*E*-**11**	14 ± 3	620 ± 80	130 ± 20
2*Z*-**11**	50 ± 7	985 ± 260	150 ± 20
2*E*-**12**	6.8 ± 0.7	180 ± 20	
2*Z*-**13**	0.3 ± 0.04	190 ± 30	

[a] Errors are standard deviations.

residues are separated by an alanine, giving rise to an EXE motif. Similar EXE motifs are found in FAH (Glu-199 and Glu-201), (*28*, *30*) as well as YcgM (Glu-72 and Glu-74). The third ligand (Asp-233 in FAH and Asp-103 in YcgM) is also present. In 4-OD, the EXE motif corresponds to Glu-109 and Glu-111, as shown in Figure 2, suggesting that these residues are important for metal binding.

Inhibition Studies. The inhibition data for the compounds synthesized in this study are summarized in Tables 2 and 3. Representative Lineweaver−Burk plots are shown in Figure 3A−C for each enzyme. Lineweaver−Burk analysis confirms the competitive nature of the inhibition. Four major trends emerge from these data. First, both series of compounds are potent inhibitors of 4-OT. In the 2-fluoro-4-alkene series, the K_i values range from 0.11 to 45 μM, with the monocarboxylated compounds (i.e., 2*E*- and 2*Z*-**8**) being the most potent inhibitors. In the 2-fluoro-4-alkyne series, the K_i values range from 0.3 to 14 μM. However, the dicarboxylated compound (i.e., 2*Z*-**13**) is the most potent inhibitor. Second, the 2*E* isomer is a more potent inhibitor than the 2*Z* isomer for the monocarboxylated compounds **8**, **9**, and **11**. For **10**, a dicarboxylated compound, the two isomers appear to be comparably potent. Unfortunately, this observation could not be explored further because it was not possible to synthesize both isomers of **13**, the other dicarboxylated inhibitor used

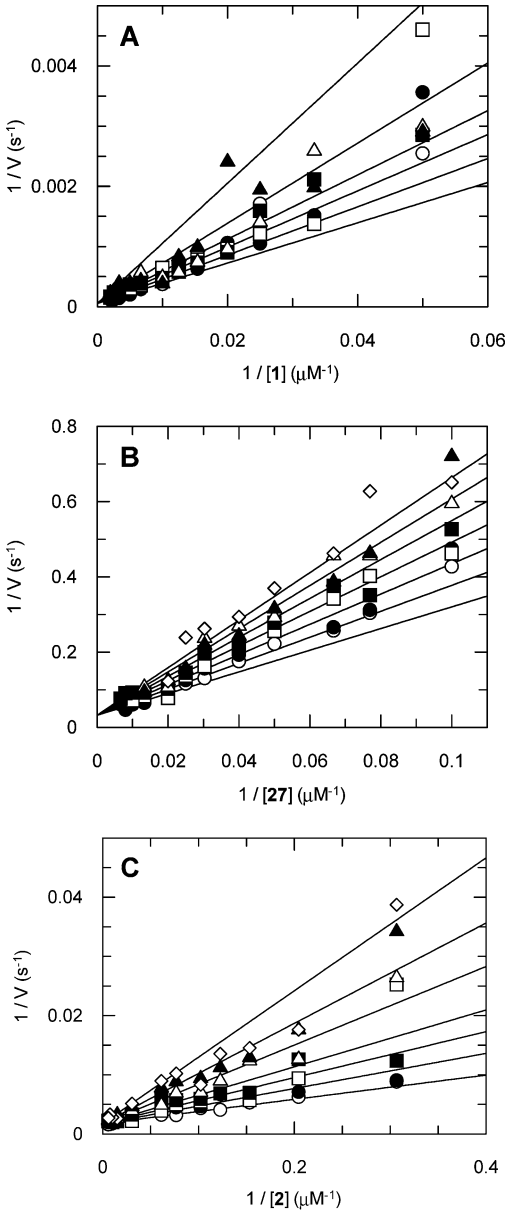

FIGURE 3: Lineweaver−Burk plots for 4-OT, YwhB, and VPH: (A) inhibition of 4-OT by varying amounts of 2*E*-**9** (○, 0 μM; ●, 0.46 μM; □, 0.91 μM; ■, 1.37 μM; △, 2.28 μM; ▲, 4.57 μM); (B) inhibition of YwhB by varying amounts of a mixture (8:1) of 2*E*/2*Z*-**10** (○, 0 μM; ●, 41.7 μM; □, 83.4 μM; ■, 125.1 μM; △, 166.8 μM; ▲, 208.5 μM; ◇, 250 μM); (C) inhibition of VPH in the E109Q-4-OD/VPH complex by varying amounts of 2*Z*-**11** (○, 0 μM; ●, 56.5 μM; □, 113 μM; ■, 169.5 μM; △, 282.5 μM; ▲, 395.5 μM; ◇, 565 μM). The experimental conditions and the inhibition constants can be found in the text.

in this study. Third, the compounds are less potent inhibitors of YwhB, having K_i values 5- to 633-fold higher than those determined for 4-OT. The 5-fold difference is observed for 2*E*/2*Z*-**10** (14:1 mixture) and the 633-fold difference is observed for 2*E*-**13**. The differences between K_i values for the other compounds range from 20- to 73-fold. Finally, 2*E*- and 2*Z*-**11** were the most potent inhibitors identified for VPH. The actual K_i values may be lower since binding of these inhibitors to the inactivated 4-OD cannot be ruled out. In view of the fact that the substrate for 4-OD is not a dienol, such a possibility seems remote. The other compounds may also inhibit VPH, but only with K_i values exceeding 500 μM. It was not possible to investigate higher concentrations because the absorbances of these compounds interfered with the UV assay of **2** at its λ_{max} of 265 nm.

DISCUSSION

Ten mono- and dicarboxylated 2-fluoro substrate analogues were synthesized and evaluated as potential inhibitors that could ultimately be used as ligands in 4-OT crystal structures. Mechanistic inferences could be made on the basis of the geometry of the enzyme−inhibitor complexes. The 10 analogues were competitive inhibitors of 4-OT with the most notable observation being their potency as assessed by the K_i values. By comparison, the K_m values for **1** (180 ± 30 μM), **2** (1100 ± 100 μM), and the dienol analogues of 2*E*- and 2*Z*-**9** (600 ± 100 μM) are considerably higher (*31*,*32*). In addition, the K_i for a previously identified competitive inhibitor of 4-OT, 2*Z*,4*Z*-muconate (**29**), is 900 ± 200 μM

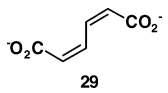

29

(*33*). If the K_m values are an approximation of the substrate's binding affinity, these differences suggest that the 2-fluoro substituent makes a significant contribution to the binding interaction between the inhibitor and the enzyme. One possible explanation for the low K_i values may involve hydrogen bonding or an electrostatic interaction between an active site residue and the fluoro group.

There are also differences in the binding interactions between 4-OT and the 2*E* and 2*Z* isomers of the monocarboxylated inhibitors, **8**, **9**, and **11**, as reflected by the different K_i values. In all cases, the 2*E*-isomer binds more tightly. Arg-11 and Arg-39 are the two most likely candidates to interact with the carboxylate group of these inhibitors, because they have been implicated in the binding of both mono- and dicarboxylated substrates by three lines of evidence. Their involvement in substrate binding was first suggested by a crystal structure of 5-(carboxymethyl)-2-hydroxymuconate isomerase (CHMI), a structurally homologous enzyme to 4-OT that processes an analogous substrate to **1**, in which a carboxymethyl group has replaced the C-5 hydrogen (*34*). In this structure, two sulfate ions are bound to the two arginines and are spaced 6.7 Å apart, a distance comparable to that between the C-1 and C-6 carboxylate groups of **1**. Second, NMR studies of 4-OT covalently bonded to 3-bromopyruvate and the enzyme as a complex with **29** showed that the chemical shifts for both Arg-11 and Arg-39 change upon the binding of **29**, while the interaction of the monocarboxylated 3-bromopyruvate with enzyme results only in changes for the chemical shifts assigned to Arg-39 (*33*). Finally, the results of mutagenesis studies have shown that replacing Arg-11 with an alanine has an impact on the binding of **1**, resulting in an 8.6-fold increase in K_m (*31*).

Assuming that the arginine residues interact with the carboxylate groups of **8**, **9**, **11**, and **12**, it is not unreasonable to envision different binding modes for these compounds, in accord with the different stereochemical fates observed for **1** and **2** (*8*). In one mode, the C-1 carboxylate interacts with Arg-39, which may also hydrogen bond to the 2-fluoro substituent. Although hydrogen bonds involving fluorocarbons are controversial, a few instances have been documented (*35*, *36*). Such interactions with the 2*E* isomers would parallel those proposed for 4-OT with its physiological substrate, **1** (*37*). The 2*Z* isomers likely cannot bind in this fashion due to their configuration and potential active site constraints. Instead, they may bind in a second mode in which Arg-11 interacts only with the carboxylate and not the fluoro substituent. In the absence of detailed structural information, these potential differences in binding remain speculative.

The second notable observation about the 4-OT inhibition data is the difference in the potency for the mono- and dicarboxylated inhibitors coupled with the reversal in potency when comparing the alkene and alkyne series. One possible explanation for this observation follows from the discussion above, in which Arg-11 and Arg-39 are major binding determinants and the monocarboxylated compounds may bind in different orientations. In this context, the presence of the additional methyl group in **9** and **12** or the linear alkyne in **11** and **12** may result in less favorable interactions, thus resulting in an increase in their respective K_i values. The dicarboxylated compounds **10** and **13** can likely interact with both arginines. It is worth noting that the K_i for **10** is ~5-fold less than the K_m for **1**, while K_i for **13** is 3 orders of magnitude less. Although the C-6 carboxylate of **13** is limited in mobility due to its alkyne moiety, the alkyl chain is longer than that of **10**. This may allow **13** to interact more favorably with Arg-11 and Arg-39, resulting in the significantly lower K_i value.

The tautomerase superfamily consists of structurally homologous proteins with two defining characteristics: they are constructed from a common building block, the $\beta-\alpha-\beta$ structural motif, and they have a catalytic amino-terminal proline (*37*, *38*). 4-OT is the best-characterized member of the 4-OT family, a group within the tautomerase superfamily. YwhB from *B. subtilis* shares 36% sequence identity with 4-OT, making it the most closely related family member to 4-OT (*22*, *37*). While the physiological function of YwhB is not known, it does not appear to be part of a degradative pathway for aromatic hydrocarbons.

YwhB shares a number of mechanistic and structural features with 4-OT as well as some intriguing differences (*2*, *37*). The results of the inhibition studies suggest further differences between 4-OT and YwhB. None of these compounds are potent inhibitors of YwhB, which is somewhat surprising in view of the fact that YwhB processes the corresponding dienols quite efficiently. For example, the YwhB-catalyzed conversion of **2** to **4** has a k_{cat}/K_m value of ~4.6×10^5 M^{-1} s^{-1} (K_m = 240 μM and k_{cat} = 112 s^{-1}) (*22*, *37*), yet the monocarboxylated 2*E*- and 2*Z*-**11** have K_i values of 620 and 985 μM, respectively. These K_i values suggest

Scheme 6

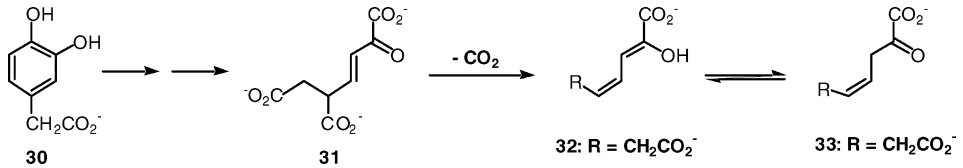

the absence of any substantial interactions between these compounds and the enzyme. The addition of a methyl group (i.e., **9** and **12**) or a carboxylate group (i.e., **10** and **13**) increases the potency (as assessed by the lower K_i values), which may reflect increased interactions with residues at the active site. Crystallographic studies to determine the reasons for the differences among K_i values within each series of inhibitors, as well as between the two proteins, are currently underway.

To assess whether the 2-fluoro substrate analogues were inhibitors of VPH, the E109Q-4-OD/VPH complex was constructed, in which the glutamine mutation inactivates 4-OD. Only the 2*E*- and 2*Z*-isomers of **11** were competitive inhibitors of VPH in the E109Q-4-OD/VPH complex. It was surprising that although these compounds were inhibitors, the 2*E*- and 2*Z*-isomers of **8** were not. Evidently, the rigidity of the linear acetylene moiety of **11** results in optimal interactions with residues in the active site; these interactions are presumably less than optimal or absent using **8**. There are currently no crystal structures available for the 4-OD/VPH complex, which precludes a determination of the structural basis for this difference.

In the course of these studies, a structure-based sequence analysis identified 4-OD as a member of the FAH superfamily, implicating Glu-109 and Glu-111 as metal binding ligands. The families within the FAH superfamily are represented by YcgM, the bacterial decarboxylase COHED, and the mouse enzyme FAH. YcgM is a putative isomerase found in *E. coli*. COHED is one of the enzymes in the homoprotocatechuate meta-fission pathway, an inducible set of enzymes in *E. coli* C that converts 3,4-dihydroxyphenylacetate (**30**, Scheme 6) to succinic semialdehyde and pyruvate (*27*). The enzymes of this pathway are part of a degradative route for phenylalanine and tyrosine, and they carry out reactions analogous to those in the catechol meta-fission pathway on substrates in which a carboxymethyl group has replaced the C-5 hydrogen of **1**. Like 4-OD, COHED catalyzes a metal-dependent decarboxylation of the vinylogous substrate, 5-(carboxymethyl)-2-oxo-3-hexene-1,6-dioate (**31**, Scheme 6) (*27*, *39*). Decarboxylation of **31** yields 2-hydroxy-2,4*Z*-heptadiene-1,7-dioate (**32**), which undergoes an enzyme-catalyzed tautomerization to afford 2-oxo-hept-4*Z*-ene-1,7-dioate (**33**) (*39*). 4-OD does not carry out an analogous tautomerization reaction on its product, **2**. FAH is part of a eukaryotic pathway responsible for the degradation of tyrosine and phenylalanine and catalyzes the last step in the pathway, which is the hydrolytic cleavage of fumarylacetoacetate to produce fumarate and acetoacetate (*28*, *30*).

Recent work uncovered a structural relationship between COHED and FAH and identified the metal binding residues in these metal-dependent enzymes (*29*). The crystal structure of a COHED·calcium complex shows that the monomeric enzyme consists of two similar halves, the N-terminal half (residues 1−200) and the C-terminal half (residues 221−449), which are connected by a short loop (residues 206−220). These two halves form a structure that is homologous to the C-terminal domain of FAH. The presence of a calcium ion in the C-terminal domain of COHED implicates this domain as the site of decarboxylation (*29*). Three residues, Glu-276, Glu-278, and Asp-307, are coordinated to the metal ion. FAH and YcgM have a similar triad of acidic residues (Glu-199, Glu-201, and Asp-233 in FAH and Glu-72, Glu-74, and Asp-103 in YcgM) which are involved in metal binding (*28*,*30*). These observations suggest that Glu-109 and Glu-111 in 4-OD are also involved in metal binding. Experiments are currently underway to verify whether these two glutamates play such a role in 4-OD.

ACKNOWLEDGMENT

We thank Steve D. Sorey (Department of Chemistry, The University of Texas at Austin) for his expert assistance in acquiring the NMR spectra.

REFERENCES

1. Dagley, S. (1978) Pathways for the utilization of organic growth substrates, in *The Bacteria: A Treatise on Structure and Function* (Ornston, L. N. and Sokatch, J. R., Eds) pp 305−388, Academic Press, New York.
2. Harayama, S., Rekik, M., Ngai, K.-L., and Ornston, L. N. (1989) Physically associated enzymes produce and metabolize 2-hydroxy-2,4-dienoate, a chemically unstable intermediate formed in catechol metabolism via *meta* cleavage in *Pseudomonas putida*. *J. Bacteriol.* **171**, 6251−6258.
3. Whitman, C. P. (1999) Keto−enol tautomerism in enzymatic reactions, in *Comprehensive Natural Products Chemistry* (Barton, D., and Nakanishi, K., Eds), Vol. 5, pp 31−50, Elsevier Science Ltd, Oxford, U.K..
4. Whitman, C. P., Aird, B. A., Gillespie, W. R., and Stolowich, N. J. (1991) Chemical and enzymatic ketonization of 2-hydroxymuconate, a conjugated enol, *J. Am. Chem. Soc. 113*, 3154−3162.
5. Lian, H., and Whitman, C. P. (1993) Ketonization of 2-hydroxy-2,4-pentadienoate by 4-oxalocrotonate tautomerase: implications for the stereochemical course and the mechanism, *J. Am. Chem. Soc. 115*, 7978−7984.
6. Stanley, T. M., Johnson, W. H., Jr., Burks, E. A., Whitman, C. P., Hwang, C.-C., and Cook, P. F. (2000) Expression and stereochemical and isotope effect studies of active 4-oxalocrotonate decarboxylase, *Biochemistry 39*, 718−726.
7. Lian, H., and Whitman, C. P. (1994) Stereochemical and isotopic labeling studies of the 4-oxalocrotonate decarboxylase/vinylpyruvate hydratase complex: analysis and mechanistic implications, *J. Am. Chem. Soc. 116*, 10403−10411.
8. Whitman, C. P., Hajipour, G., Watson, R. J., Johnson, W. H., Jr., Bembenek, M. E., and Stolowich, N. J. (1992) Stereospecific ketonization of 2-hydroxymuconate by 4-oxalocrotonate tautomerase and 5-(carboxymethyl)-2-hydroxymuconate isomerase, *J. Am. Chem. Soc. 114*, 10104−10110.
9. Almrud, J. J., Kern, A. D., Wang, S. C., Czerwinski, R. M., Johnson, W. H., Jr., Murzin, A. G., Hackert, M. L., and Whitman, C. P. (2002) The crystal structure of YdcE, a 4-oxalocrotonate tautomerase homologue from *Escherichia coli*, confirms the structural basis for oligomer diversity, *Biochemistry 41*, 12010−12024.
10. Czerwinski, R. M., Johnson, W. H., Jr., Whitman, C. P., Harris, T. K., Abeygunawardana, C., and Mildvan, A. S. (1997) Kinetic

and structural effects of mutations of the catalytic amino-terminal proline in 4-oxalocrotonate tautomerase, *Biochemistry 36*, 14551−14560.
11. Sambrook, J., Fritsch, E. F., and Maniatis, T. (1989) *Molecular Cloning: A Laboratory Manual*, Cold Spring Harbor Laboratory, Cold Spring Harbor, NY.
12. Waddell, W. J. (1956) A simple ultraviolet spectrophotometric method for the determination of protein, *J. Lab. Clin. Med. 48*, 311−314.
13. Laemmli, U. K. (1970) Cleavage of structural proteins during the assembly of the head of bacteriophage T4, *Nature 227*, 680−685.
14. Altschul, S. F., Madden, T. L., Schäffer, A. A., Zhang, J., Zhang, Z., Miller, W., and Lipman, D. J. (1997) Gapped BLAST and PSI−BLAST: a new generation of protein database search programs, *Nucleic Acids Res. 25*, 3389−3402.
15. Thompson, J. D., Higgins, D. G., and Gibson, T. J. (1994) CLUSTAL W: improving the sensitivity of progressive multiple sequence alignment through sequence weighting, position-specific gap penalties and weight matrix choice, *Nucleic Acids Res*. *22*, 4673−4680.
16. Ho, S. N., Hunt, H. D., Horton, R. M., Pullen, J. K., and Pease, L. R. (1989) Site-directed mutagenesis by overlap extension using the polymerase chain reaction, *Gene 77*, 51−59.
17. Burks, E. A., Johnson, W. H., Jr., and Whitman, C. P. (1998) Stereochemical and isotopic labeling studies of 2-oxo-hept-4-ene-1,7-dioate hydratase: evidence for an enzyme-catalyzed ketonization step in the hydration reaction, *J. Am. Chem. Soc. 120*, 7665−7675.
18. Etemad-Moghadam, G., and Seyden-Penne, J. (1985) Synthèse stéréosélective d'esters α,*β*-éthyléniques α-fluorés *E* par réaction de Wittig-Horner à partir du diéthyl phophono α-fluoroacétate de méthyle Etude comparative avec le diphényl phophonoxy α-fluoroacétate de méthyle, *Bull. Soc. Chim. Fr.*, 448−454.
19. Landor, S. R., Landor, P. D., and Kalli, M. (1983) The synthesis of a cyclopropane amino acid, trans-α-(carboxycyclopropyl)glycine, found in ackee seed, *J. Chem. Soc., Perkin Trans. 1*, 2921−2925.
20. Rabjohn, N. (1963) Propiolaldehyde, *Org. Synth. Collect. 4*, 813−815.
21. Dunn, P. J., and Rees, C. W. (1987) Organic heterocyclothiazenes. Part 5. Cycloaddition reactions of tetrasulphur tetranitride with highly electron deficient alkynes, *J. Chem. Soc., Perkin Trans. 1*, 1579−1584.
22. Wang, S. C, Johnson, W. H., Jr., Czerwinski, R. M., and Whitman, C. P. (2004) Reactions of 4-oxalocrotonate tautomerase and YwhB with 3-halopropiolic acids: analysis and implications, *Biochemistry 43*, 748−758.
23. Thenappan, A., and Burton, D. J. (1990) Alkylation of (fluorocarbethoxymethylene)tri-*n*-butylphosphorane: a facile entry to α-fluoroalkanoates, *J. Org. Chem. 55*, 2311−2317.
24. Pirrung, M. C., Chen, J., Rowley, E. G., and McPhail, A. T. (1993) Mechanistic and stereochemical study of phenylpyruvate tautomerase, *J. Am. Chem. Soc. 115*, 7103−7110.
25. Thenappan, A., and Burton, D. J. (1990) Reduction-olefination of esters: a new and efficient synthesis of α-fluoro α, *β*-unsaturated esters, *J. Org. Chem. 55*, 4639−4642.
26. Kaschabek, S. R., and Reineke, W. (1994) Synthesis of bacterial metabolites from haloaromatic degradation. 1. Fe(III)-catalyzed peracetic acid oxidation of halocatechols, a facile entry to *cis*, *cis*-2-halo-2,4-hexadienedioic acids and 3-halo-5-oxo-2(5*H*)-furanylideneacetic acids, *J. Org. Chem. 59*, 4001−4003.
27. Garrido-Pertierra, A., and Cooper, R. A. (1981) Identification and purification of distinct isomerase and decarboxylase enzymes involved in the 4-hydroxyphenylacetate catabolic pathway of *Escherichia coli*, *Eur. J. Biochem. 117*, 581−584.
28. Timm, D. E., Mueller, H. A., Bhanumoorthy, P., Harp, J. M. and Bunick, G. J. (1999) Crystal structure and mechanism of a carbon−carbon bond hydrolase, *Structure 7*, 1023−1033.
29. Tame, J. R. H., Namba, K., Dodson, E. J., and Roper, D. I. (2002) The crystal structure of HpcE, a bifunctional decarboxylase/isomerase with a multifunctional fold, *Biochemistry 41*, 2982−2989.
30. Bateman, R. L., Bhanumoorthy, P., Witte, J. F., McClard, R. W., Grompe, M., and Timm, D. E. (2001) Mechanistic inferences from the crystal structure of fumarylacetoacetate hydrolase with a bound phosphorus-based inhibitor, *J. Biol. Chem. 276*, 15284−15291.
31. Harris, T. K., Czerwinski, R. M., Johnson, W. H., Jr., Legler, P. M., Abeygunawardana, C., Massiah, M. A., Stivers, J. T., Whitman, C. P., and Mildvan, A. S. (1999) Kinetic, stereochemical, and structural effects of mutations of the active site arginine residues in 4-oxalocrotonate tautomerase, *Biochemistry 38*, 12343−12357.
32. Lian, H., Czerwinski, R. M., Stanley, T. M., Johnson, W. H., Jr., Watson, R. J., and Whitman, C. P. (1998) The contribution of the substrate's carboxylate group to the mechanism of 4-oxalocrotonate tautomerase, *Bioorg. Chem. 26*, 141−156.
33. Stivers, J. T., Abeygunawardana, C., Mildvan, A. S., and Whitman, C. P. (1996) ^{15}N NMR relaxation studies of free and inhibitor-bound 4-oxalocrotonate tautomerase: backbone dynamics and entropy changes of an enzyme upon inhibitor binding, *Biochemistry 35*, 16036−16047.
34. Subramanya, H. S., Roper, D. I., Dauter, Z., Dodson, E. J., Davies, G. J., Wilson, K. S., and Wigley, D. B. (1996) Enzymatic ketonization of 2-hydroxymuconate: specificity and mechanism investigated by the crystal structures of two isomerases, *Biochemistry 35*, 792−802.
35. Dunitz, J. D., and Taylor, R. (1997) Organic fluorine hardly ever accepts hydrogen bonds, *Chem.−Eur. J. 1*, 89−98.
36. Barbarich, T. J., Rithner, C. D., Miller, S. M., Anderson, O. P., and Strauss, S. H. (1999) Significant inter- and intramolecular O−H F−C Hydrogen Bonding, *J. Am. Chem. Soc. 121*, 4280−4281.
37. Whitman, C. P. (2002) The 4-oxalocrotonate tautomerase family of enzymes: how nature makes new enzymes using a *β*−α−*β* structural motif, *Arch. Biochem. Biophys. 402*, 1−13.
38. Poelarends, G. J., Serrano, H., Person, M. D., Johnson, W. H., Jr., Murzin, A. G., and Whitman, C. P. (2004) Cloning, expression, and characterization of a *cis*-3-chloroacrylic acid dehalogenase: insights into the mechanistic, structural, and evolutionary relationship between isomer-specific 3-chloroacrylic acid dehalogenases, *Biochemistry 43*, 759−772.
39. Johnson, Jr., W. H., Hajipour, G., and Whitman, C. P. (1995) The stereochemical course of 5-(carboxymethyl)-2-oxo-3-hexene-1,6-dioate decarboxylase from *Escherichia coli C*, *J. Am. Chem. Soc. 117*, 8719−8726.

BI049489P